Attenuated total reflectivity of semiconductors with wave-vector-linear band splitting

P. Halevi
Departmento de Fisica del Instituto de Ciencias, Universidad Autonoma de Puebla, Puebla 72570, Mexico

Olivier B. M. Hardouin Duparc
Laboratoire de Physique des Materiaux, Centre National de la Recherche Scientifique, 1 Place A. Briand, 92195 Meudon, Principal Cedex

A. A. Maradudin and R. F. Wallis
Department of Physics, University of California, Irvine, California 92717
(Received 21 October 1986)

We have calculated the attenuated total reflectivity (ATR) of a semiconductor near an excitonic transition in the presence of wave-vector-linear energy-band splitting. The numerical work corresponds to the $B(n=1)$ exciton of CdS, the light being p(TM) polarized in a plane perpendicular to the crystal axis. The ATR spectra reveal two minima: One is a broad minimum between ω_T and ω_L (the transverse and longitudinal exciton frequencies) and the other is a narrow minimum at $\sim\omega_T$. These resonances are interpreted as corresponding, respectively, to the ordinary (essentially local) surface-exciton-polariton and to a new ("nonlocal") surface mode.

I. INTRODUCTION

Surface-exciton-polaritons in semiconductors with parabolic energy bands have been extensively studied in the past 10 years. In the present work we study surface polaritons in the presence of energy-band splitting which is linear in the wave vector. We focus on the calculation of attenuated total reflectvity (ATR) spectra of the B exciton of CdS, which is the prototype of this kind of nonparabolic dispersion.

Energy bands in direct-gap semiconductors are often isotropic and the energies of the corresponding excitons are adequately described by means of a parabolic relation,

$$\hbar\omega_T(q)=\hbar\omega_T(0)+\hbar^2q^2/2m \ ,$$

where $\mathbf{q}$ is the wave vector and m is the mass of the exciton. In uniaxial crystals, however, a crystal field E_c may exist in the direction of the axis $\hat{\mathbf{c}}(||\hat{\mathbf{y}})$. This field is perceived by a moving electron as a magnetic field in the xz plane and gives rise to a spin-orbit coupling of the form

$$H'=\phi(q_z\sigma_y-q_x\sigma_x) \ .$$

Here $q_{x,z}$ are the transverse components of the wave vector, $\sigma_{x,y}$ are the Pauli matrices (in the usual notation), and ϕ is a parameter that is proportional to the crystal field E_c. The combined effect of the electron in the conduction band and hole in the valence band leads to the following eigenvalues for the exciton

$$\begin{aligned}\hbar\omega_{\pm}(\mathbf{q})&=\hbar\omega_T(0)+\frac{\hbar^2}{2m_\perp}(q_x^2+q_z^2)+\frac{\hbar^2}{2m_{||}}q_y^2\pm\phi(q_x^2+q_z^2)^{1/2}\\&=\hbar\omega_T(0)+\frac{\hbar^2}{2m_{||}}q_y^2\\&\quad+\frac{\hbar^2}{2m_\perp}\left[q_\perp\pm\frac{m_\perp\phi}{\hbar^2}\right]^2-\frac{m_\perp\phi^2}{2\hbar^2} \ ,\end{aligned}$$

where $m_\perp$ and $m_{||}$ are the transverse and longitudinal masses and $q_\perp=(q_x^2+q_z^2)^{1/2}$ is the wavevector component perpendicular to the $\hat{\mathbf{c}}$ axis. This heuristic derivation is best applicable to the $B(n=1)$ exciton of CdS. This exciton is composed of a hole in the second (out of three) valence band and an electron in the conduction band, both with Γ_7 symmetry.

The last equation for $\hbar\omega_{\pm}(\mathbf{q})$ tells us that the spin-orbit interaction has produced a splitting of the original exciton band into two bands whose minima are separated in phase space by $\Delta q=2m_\perp\phi/\hbar^2$. As this effect is proportional to ϕ, we will refer to ϕ as the "exciton-splitting" or "q-linear-splitting" parameter. Clearly, there is no effect for $\mathbf{q}||\hat{\mathbf{c}}$ and therefore it is simplest to study the case $\mathbf{q}\perp\hat{\mathbf{c}}$. This is to say that, in optical studies, the plane of incidence is chosen perpendicular to the $\hat{\mathbf{c}}$ axis, and so, the crystal must be cleaved in a plane that is parallel to this axis. If, in addition, the electric field of the incident wave is polarized in a plane that is perpendicular to $\hat{\mathbf{c}}$ ($\mathbf{E}\perp\hat{\mathbf{c}}$, that is p-polarized light), then the perturbation H' couples a dipole-forbidden to a dipole-allowed optical transition, and both turn out to have equal oscillator strengths; their energies are given by the above formula for $\hbar\omega_{\pm}(\mathbf{q})$. On the other hand, while coupling between an allowed and a forbidden transition also exists for $\mathbf{E}||\hat{\mathbf{c}}$, in the case of CdS this coupling is too weak to cause an appreciable transfer of oscillator strength from the allowed to the forbidden state. For this reason the wave-vector-linear effects are not observed for $\mathbf{E}||\hat{\mathbf{c}}$, that is, for s-polarized light.

In 1964 a shoulder detected in the normal-incidence reflectivity of the B $(n=1)$ exciton of CdS for $\mathbf{q}\perp\hat{\mathbf{c}}$ with $\mathbf{E}\perp\hat{\mathbf{c}}$ led Mahan and Hopfield[1] to develop a theory of this spectrum that was based on q-linear energy terms permitted by the wurtzite crystal symmetry of CdS. This pioneering work successfully reproduced the shoulder and, moreover, accounted for the absence of any effect in CdS

for $\mathbf{q}\|\hat{\mathbf{c}}$ and $\mathbf{q}\perp\hat{\mathbf{c}}$ with $\mathbf{E}\|\hat{\mathbf{c}}$. However, Mashlyatina *et al.*[2] found that β-AgI—another wurtzite crystal—does exhibit an "anomalous" spectrum for $\mathbf{q}\perp\hat{\mathbf{c}}$ with $\mathbf{E}\|\hat{\mathbf{c}}$. It seems that for this semiconductor, unlike for CdS, a strong coupling between an allowed and a forbidden transition causes a "flareup" of the latter.

The two split-exciton branches introduced in Ref. 1, when coupled to light, give rise to three transverse-mode polariton branches, rather than the usual two branches that exist in the presence of spatial dispersion (in the cases of the A- and C-exciton series).[3] The advent of resonant Brillouin scattering[4] in 1977 led to the attractive possibility of a direct detection of the additional branch of the B exciton. Indeed, this was proposed by Allen and Kane[5] and, independently, Koteles and Winterling[6] observed acoustic phonon scatterings corresponding to three polariton branches. These authors also raised a doubt about attributing the q-linear splitting to spin-orbit coupling. The investigation of exciton-polaritons by means of laser techniques has been reviewed by Koteles.[7]

It was thought that q-linear terms may be safely ignored for A excitons, because such terms are forbidden by symmetry for the uppermost valence band (from which this series derives) and they are known to be negligible for the conduction band. Nevertheless, recently a very fine splitting of one of the polariton branches has been observed by Lu *et al.*[8] The effect is significant only in the vicinity of the crossing point of two theoretically derived branches. The splitting parameter ϕ of the A exciton was found to be about thirty times smaller than that of the B exciton. On the other hand, the q-linear term turned out to affect in an important way the Brillouin linewidth, leading to a frequency-dependent damping constant.[9]

Generalizing the treatment of Ref. 1, Thang and Fishman[10] have derived the Hamiltonians of the A and B excitons of CdS, taking into account the longitudinal-transverse splitting and the exchange energy. They were also able to show that experimentally deduced parameters for the A exciton provide the parameters for the B excitons.

The application of a static magnetic field H_0 lowers the symmetry of the system, and the band-structure calculation becomes much more complicated. The bands exhibit Zeemann splitting and the optical spectra display new features. A detailed study of the A and B excitons of CdS and ZnO for $H_0\neq 0$ (as well as $H_0=0$) has been undertaken by Blattner *et al.*[11] These authors derived the Hamiltonian, solved the eigenvalue problem and obtained the exciton-polariton modes. From a comparison with a variety of experimental results (two-photon Raman scattering, transmission, and reflection in magnetic fields up to 20 T) they deduced the numerical values of the A- and B-exciton parameters. More recently Rosenzweig[12] studied the magnetoreflectance of the B exciton of CdS in other configurations.

One manifestation of natural optical activity[13] is a change in the polarization of the incident wave, observed in the polarization of the reflected wave. Ivchenko *et al.*[14] experimented with oblique incidence of light in the vicinity of the B ($n=1$) exciton of CdS. When the incident light was p (s) polarized the reflected light turned out to have an s (p)-polarized component, in addition to the usual p (s)-polarized component. The cross-reflection coefficients ($r_{ps}=r_{sp}$) are peaked at the longitudinal exciton frequency ω_L and, at the peak value, $r_{ps}/r_{pp}\sim r_{sp}/r_{ss}\sim 0.04$. The effect is well accounted for[15] by superposing all four states that contribute to the B exciton.[16] The anisotropic behavior is caused by the appearance of off-diagonal elements in the dielectric tensor; these elements are proportional to q_x and q_z. The natural optical activity was also manifest in ellipsometric investigations[17] and in the luminescence spectrum[18] of CdS. Spatial dispersion effects in the exciton resonance region have been reviewed by Ivchenko.[19]

In addition to the wurtzite symmetry there are other uniaxial symmetries that admit wave-vector-linear energy bands. As pointed out by Bishop and Maradudin,[20] in crystals of D_3 symmetry a band splitting occurs that is linear in the component q_y, rather than in the transverse components. In crystals of zinc-blende symmetry the q-linear effect is overshadowed by the valence-band splitting into light- and heavy-hole bands.[21]

The present work deals with semiconductors which have the wurtzite symmetry and is *not* applicable to crystals of D_3 or zinc-blende symmetries. We employ the original, isotropic model of Mahan and Hopfield,[1] that is, we neglect the off-diagonal elements of the dielectric tensor[14–19] on account of their smallness. Our principal interest lies in the attenuated total reflectivity (ATR) spectra of the B ($n=1$) exciton of CdS. In a preliminary communication[22] we called attention to the existence of two ATR minima, instead of one, as is usual. The additional minimum appears in the vicinity of ω_T and vanishes in the limit $\phi\rightarrow 0$. We have suggested that this minimum corresponds to a new surface polariton mode. This possibility will be explored in greater detail in the following sections.

ATR spectroscopy implies p-polarized light, and thus we must consider longitudinal, as well as transverse modes. There are three transverse modes, essentially the same as for normal incidence.[1,5] In addition, now there are two new, longitudinal modes. The five bulk-polariton branches are analyzed in Sec. II. In Sec. III we generalize the additional boundary conditions (ABC's) employed by Mahan and Hopfield, to the case of p polarization and we calculate the surface impedance of the semiconductor, with allowance for an exciton-free ("dead") layer. This leads to our final expression for the ATR spectrum in Sec. IV. An analysis of various spectra is presented in Sec. V and we summarize our conclusions in Sec. VI.

II. BULK MODES

As stated in the Introduction, the wave-vector-linear band splitting in wurtzite-type semiconductors is observed if both the wave vector and the electric field are perpendicular to the uniaxial crystalline axis $\hat{\mathbf{c}}$, chosen along the y axis ($\mathbf{q}\perp\hat{\mathbf{c}},\mathbf{E}\perp\hat{\mathbf{c}}$). According to the condition $\mathbf{q}\perp\hat{\mathbf{c}}$ the plane of incidence must be normal to $\hat{\mathbf{c}}$, which is to say that the crystal must be cleaved in a plane that is parallel to $\hat{\mathbf{c}}$. The condition $\mathbf{E}\perp\hat{\mathbf{c}}$ requires the electric field to be parallel to the plane of incidence (the xz plane) corre-

sponding to p(TM)-polarized waves. This, of course, is just the polarization for which surface polariton modes may exist in nonmagnetic crystals.

In our geometry $q_y=0$ and $E_y=0$. Therefore the problem is essentially isotropic and the semiconductor may be characterized by a scalar dielectric function $\epsilon(\omega,q)$, where ω is the circular frequency and $q=(q_x^2+q_z^2)^{1/2}$ is the wave vector. According to the Mahan-Hopfield model[1] the oscillator-strength $4\pi\beta$ is equally divided among the excitons with eigenvalues $\hbar\omega_+(q)$ and $\hbar\omega_-(q)$, giving rise to the dielectric function

$$\epsilon(\omega,q)=\epsilon_0+\frac{2\pi\beta\omega_T^2}{\omega_+^2(q)-\omega^2-i\nu\omega}+\frac{2\pi\beta\omega_T^2}{\omega_-^2(q)-\omega^2-i\nu\omega}\ , \quad (1)$$

where

$$\hbar\omega_\pm(q)=\hbar\omega_T+\hbar^2q^2/2m_\perp\pm\phi q\ . \quad (2)$$

Here ϵ_0 is the background dielectric constant, $4\pi\beta$ is the oscillator strength of the unsplit exciton, $\omega_T\equiv\omega_T(0)$ is the resonance frequency of the exciton, ν is a phenomenological damping frequency, $m_\perp$ is the transverse exciton mass, and ϕ is the exciton-splitting parameter. The second and the third terms in Eq. (1) describe, respectively, the contributions of the split "+" and "−" excitons whose energies are given by Eq. (2). In the limit $\phi\to0$ Eq. (1) reduces to the dielectric function in the Hopfield-Thomas model,[3] applicable to many direct-gap semiconductors.

The second and third terms in Eq. (2) are very small compared to the first term and the following is a good approximation:

$$\omega_\pm^2(q)\simeq\omega_T^2+Dq^2\pm\Phi q\ , \quad (3)$$

where $D=\hbar\omega_T/m_\perp$ and $\Phi=2\omega_T\phi/\hbar$. The substitution of Eq. (3) into Eq. (1) simplifies the dielectric function substantially,

$$\epsilon(\omega,q)=\epsilon_0-\frac{4\pi\beta\omega_T^2(\Omega^2-Dq^2)}{\Omega^4-(2D\Omega^2+\Phi^2)q^2+D^2q^4}\ , \quad (4)$$

where

$$\Omega^2=\omega^2-\omega_T^2+i\nu\omega\ . \quad (5)$$

Because our fields are p polarized, longitudinal as well as transverse bulk modes will be excited. The transverse modes must satisfy the equation

$$\epsilon(\omega,q)=q^2c^2/\omega^2\ . \quad (6)$$

The substitution of Eq. (4) in Eq. (6) leads to an equation that is cubic in q^2, namely,

$$D^2q^6-(2D\Omega^2+\epsilon_0D^2q_0^2+\Phi^2)q^4+(\Omega^4-4\pi\beta\omega_T^2Dq_0^2+2\epsilon_0D\Omega^2q_0^2+\epsilon_0\Phi^2q_0^2)q^2+(4\pi\beta\omega_T^2-\epsilon_0\Omega^2)\Omega^2q_0^2=0,\quad q_0=\omega/c\ . \quad (7)$$

In the limit $q\to0$ and neglecting ν there are three solutions: $\omega=qc\epsilon_0^{-1/2}\omega_T/\omega_L$, $\omega=\omega_T$, and $\omega=\omega_L$, where $\omega_L=\omega_T(1+4\pi\beta/\epsilon_0)^{1/2}$ is the longitudinal exciton frequency. The three corresponding polariton branches are well established. The lowest branch first follows the light line and then, for $\omega\gtrsim\omega_T$, one of the split bare-exciton parabolas. The minimum of the second branch is located at ω_T, and that of the highest branch at ω_L.

If we neglect the damping frequency ν in Eq. (5) then the coefficients of the four terms of Eq. (7) are all real. Then, depending on the sign of the discriminant of the cubic equation, the three solutions for q^2 are either all real quantities, or else one solution is real and the other two are complex conjugates of each other. This is still true for q_z^2 because the wave-vector component q_x (taken in a direction parallel to the surface) is real. The sign of the roots q_z is determined by the requirement that the fields may not diverge as $z\to+\infty$; therefore we must have $\mathrm{Im}q_z\geq0$. The conclusion is that, depending on the spectral region, q_z may have the form α, or $i\gamma$, or (in pairs) $\pm\delta+i\lambda$, where α, γ, δ, and λ are positive functions of ω.

Next, we turn to the longitudinal bulk modes. Their dispersion relations are given by

$$\epsilon(\omega,q)=0\ . \quad (8)$$

Substituting Eq. (4) in Eq. (8) we get a biquadratic equation,

$$\epsilon_0D^2q^4-(2\epsilon_0D\Omega^2-4\pi\beta\omega_T^2D+\epsilon_0\Phi^2)q^2+\Omega^2(\epsilon_0\Omega^2-4\pi\beta\omega_T^2)=0\ . \quad (9)$$

From an analysis that is analogous to that for the transverse modes it follows that the two longitudinal solutions for q_z have the same analytic behavior, that is α, or $i\gamma$, or $\pm\delta+i\lambda$. It is easy to show that, for

$$\omega^2>\omega_T^2-(\epsilon_0\Phi^2-4\pi\beta\omega_T^2D)^2/4\epsilon_0^2D\Phi^2\ ,$$

q_z must have either one of the forms α or $i\gamma$. In the limit $q\to0$, Eq. (9) has the solutions $\omega=\omega_T$ and $\omega=\omega_L$, just like two of the transverse branches.

In this paper our interest lies in the ATR spectroscopy, so we have to introduce an auxiliary prism (index n_p). If the internal angle of incidence is θ_0 then the parallel wave-vector component is $q_x=q_0n_p\sin\theta_0$, and the normal component in the semiconductor is

$$q_z=(q^2-q_0^2n_p^2\sin^2\theta)^{1/2},\quad \mathrm{Im}q_z\geq0\ . \quad (10)$$

As discussed above, there are three transverse-wave solutions for q^2, and they are given by Cardan's solution of Eq. (7). The corresponding values of q_z, Eq. (10), are labeled q_1, q_2, and q_3. The two longitudinal-wave solutions

for q^2 are calculated from Eq. (9) and substituted in Eq. (10). The resulting values of q_z are denoted by q_4 and q_5.

We have calculated the real and imaginary parts of the normal components q_i of the five modes for the B exciton of CdS. The parameters used in the calculation are[6] $\epsilon_0=7.2$, $\omega_T=20\,712.3$ cm^{-1}, $\omega_{LT}\equiv\omega_L-\omega_T=10.1$ cm^{-1}, $\hbar\nu=7.5\times10^{-5}$ eV, $m=1.2m_0$, where m_0 is the free-electron mass, and $\phi=5.6\times10^{-12}$ eV m. Note that

$$4\pi\beta/\epsilon_0=\omega_L^2/\omega_T^2-1\simeq2\omega_{LT}/\omega_T\sim10^{-3}\,, \tag{11}$$

and that 1 cm$^{-1}\simeq1.24\times10^{-4}$ eV. We also take $n_p=1.5$ and $\theta_0=70°$. The results of the calculation are plotted in Fig. 1. We see that, except in the vicinity of ω_T and ω_L, the analytic behavior of the q_i conforms with the results of our previous analysis. For $\omega\simeq\omega_T$ and $\omega\simeq\omega_L$ our allowance for a finite damping frequency ν has an important effect, as is also the situation for the A excitons. Ignoring these regions q_1 is essentially real, so the partial mode $i=1$ is a real, transverse wave. We notice that the dispersion of this mode is very similar to that of the "nonlocal mode" of the A exciton. Well below ω_T the modes $i=2$ and 3 exhibit the behavior $q_{2,3}\simeq\pm\delta+i\lambda$. The fact that the mode 3 is outgoing (Re$q_3<0$) is a result of the necessary choice Im$q_3\geq0$. Clearly, this partial mode (or, for that matter, any other partial mode) does not have a separate physical existence; what really matters is that the total fields (composed of the five partial fields) do not diverge. Between ω_T and ω_L mode 2 becomes real, while mode 3 is evanescent (q_3 is pure imaginary). Well above ω_L both modes are real. As for the longitudinal modes, interestingly, the behavior of $q_4(q_5)$ is qualitatively the same as that of the transverse wave-vector component q_2 (q_3).

We also notice from Fig. 1 that, generally speaking, all the q_i are one order of magnitude greater than $q_0\simeq\omega_T/c$. This explains, partially, the importance of the nonlocal effects in the present case. The other part of the explanation lies in a study of the amplitudes of the five partial modes.

III. ADDITIONAL BOUNDARY CONDITIONS (ABC) AND SURFACE IMPEDANCE

Following Mahan and Hopfield[1] we assume that the spatially dispersive medium is bounded by an exciton-free surface layer. This "dead layer," of width l, is characterized by the background dielectric constant ϵ_0. The wave fields are simple superpositions of forward- and backward-going plane waves:

$$E_x^{(l)}(\mathbf{r},t)=(E_x^{(+)}e^{iq_lz}+E_x^{(-)}e^{-iq_lz})e^{i(q_xx-\omega t)}\,, \tag{12}$$

$$B_y^{(l)}(\mathbf{r},t)=\frac{q_0\epsilon_0}{q_l}(E_x^{(+)}e^{iq_lz}-E_x^{(-)}e^{-iq_lz})e^{i(q_xx-\omega t)}\,, \tag{13}$$

where $q_l=(q_0^2\epsilon_0-q_x^2)^{1/2}$ is the normal component of the wave vector in the exciton-free layer and $E_x^{(+)}$ and $E_x^{(-)}$ are undetermined amplitudes. Equation (13) is readily deduced from Eq. (12) using Faraday's law.

In the spatially dispersive bulk the fields are expressed as superpositions of the five partial plane-wave bulk modes:

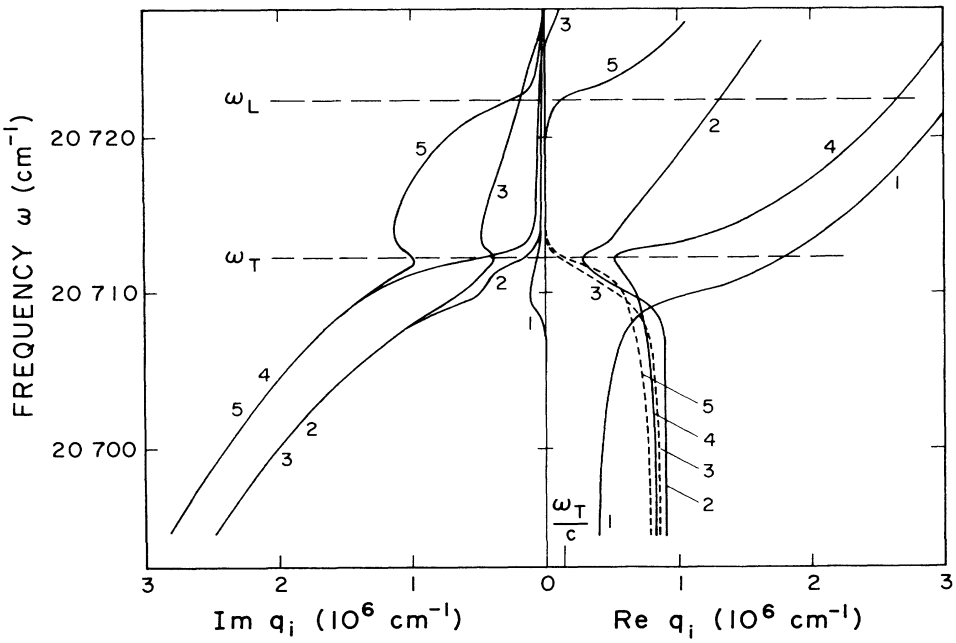

FIG. 1. Dispersion relations $\omega(q_z)$ for the five partial bulk modes of the B exciton of CdS. Req_i and Imq_i are plotted, respectively, to the right and to the left of the origin. The modes 1, 2, and 3 are transverse, and the longitudinal modes 4 and 5 arise because the fields are p polarized (angle of incidence $\theta_0=70°$). The dashed lines indicate that, in the corresponding spectral region, Re$q_{3,5}$ are negative. The parameters (Ref. 6) are listed in Sec. II.

$$E_x(\mathbf{r},t)=\left[\sum_{k=l}^{5}E_x^{(k)}e^{iq_kz}\right]e^{i(q_xx-\omega t)}, \tag{14}$$

$$B_y(\mathbf{r},t)=\left[\sum_{k=1}^{3}\frac{q_0\epsilon_k}{q_k}E_x^{(k)}e^{iq_kz}\right]e^{i(q_xx-\omega t)}. \tag{15}$$

The last expression is derived from the x component of Maxwell's equation $\nabla\times\mathbf{B}=(1/c)\partial\mathbf{D}/\partial t$. The notation ϵ_k is an abbreviation for $\epsilon(\omega,q_k)$. By Eq. (8) this function vanishes for the longitudinal modes, that is, $\epsilon_4=\epsilon_5\equiv 0$. This is why, in Eq. (15), the summation has been curtailed at $k=3$, reflecting the fact that a longitudinal electric field is *not* accompanied by a magnetic field.

We choose the plane $z=0$ as the interface between the dead layer and the nonlocal bulk ($z>0$). Then the crystalline surface lies in the plane $z=-l$. The optical properties may be conveniently expressed in terms of a surface impedance, defined as

$$Z_p=E_x(z=-l^+)/B_y(z=-l^+), \tag{16}$$

where by $-l^+$ we mean "just inside the medium." By substituting Eqs. (12) and (13) in Eq. (16) we easily find that

$$Z_p=\frac{q_l}{q_0\epsilon_0}\frac{1+\exp(2iq_ll)E_x^{(-)}/E_x^{(+)}}{1-\exp(2iq_ll)E_x^{(-)}/E_x^{(+)}}. \tag{17}$$

The next step is applying the conditions of the continuity of E_x and B_y at the interface $z=0$. Using Eqs. (12)—(15) we find that

$$Z_p=\frac{q_l}{q_0\epsilon_0}\frac{\rho-i\tan(q_ll)}{\tan(q_ll)-i\rho}, \tag{18}$$

where

$$\rho=\frac{\epsilon_0}{q_l}\sum_{k=1}^{5}E_x^{(k)}\Big/\sum_{k=1}^{3}\frac{\epsilon_k}{q_k}E_x^{(k)}$$
$$=\epsilon_0\frac{1+E_x^{(2)}/E_x^{(1)}+E_x^{(3)}/E_x^{(1)}+E_x^{(4)}/E_x^{(1)}+E_x^{(5)}/E_x^{(1)}}{\epsilon_1q_l/q_1+\epsilon_2(q_l/q_2)(E_x^{(2)}/E^{(1)})+\epsilon_3(q_l/q_3)(E_x^{(3)}/E^{(1)})}. \tag{19}$$

We have thus expressed the surface impedance of the medium in terms of the four amplitudes $E_x^{(2)}$, $E_x^{(3)}$, $E_x^{(4)}$, and $E_x^{(5)}$, rationalized to the amplitude $E_x^{(1)}$. We need four ABC's in order to determine these amplitude ratios. This is as it should be because there are five modes, compared to a single mode in the absence of spatial dispersion. Mahan and Hopfield,[1] considering only normal incidence, assumed that the polarizations $P_x^{(+)}$ and $P_x^{(-)}$ of the two split excitons vanish at the interface between the nonlocal bulk and the exciton-free layer. In the present case of p polarization these conditions have to be supplemented by the requirement that $P_z^{(+)}$ and $P_z^{(-)}$ also vanish at $z=0^+$. These polarizations are expressed in terms of a superposition of normal modes, that is, the four ABC's are

$$\sum_{k=1}^{5}\chi^{(+)}(q_k)E_x^{(k)}=0,\quad \sum_{k=1}^{5}\chi^{(-)}(q_k)E_x^{(k)}=0, \tag{20}$$

$$\sum_{k=1}^{5}\chi^{(+)}(q_k)E_z^{(k)}=0,\quad \sum_{k=1}^{5}\chi^{(-)}(q_k)E_z^{(k)}=0, \tag{21}$$

where $\chi^{(\pm)}(q_k)$ are the susceptibilities of the split modes. By Eqs. (1), (3), and (11) they are given by

$$\chi^{(\pm)}(q_k)=\frac{(\frac{1}{2})\beta\omega_T^2}{\omega_\pm^2(q_k)-\omega^2-i\nu\omega} \tag{22}$$

$$=\frac{(\epsilon_0/4\pi)\omega_T\omega_{LT}}{D(q_x^2+q_k^2)\pm\Phi(q_x^2+q_k^2)^{1/2}-\Omega^2}. \tag{23}$$

The three transverse modes must satisfy the equation $\nabla\cdot\mathbf{E}^{(k)}=0$, that is, $q_xE_x^{(k)}+q_kE_z^{(k)}=0$. For the two longitudinal modes we have $\nabla\times\mathbf{E}^{(k)}=\mathbf{0}$, or $q_xE_z^{(k)}-q_kE_x^{(k)}=0$. This allows us to express the normal components of the electric fields in terms of the parallel components, as follows:

$$E_z^{(k)}=\gamma_kE_x^{(k)}, \tag{24}$$

where

$$\gamma_k=\begin{cases}-q_x/q_k, & k=1,2,3\\ q_k/q_x, & k=4,5.\end{cases} \tag{25}$$

Then we may rewrite Eqs. (20) and (21) in the compact form

$$\sum_{k=1}^{5}A_{jk}E_x^{(k)}=0,\quad j=1,2,3,4, \tag{26}$$

with

$$A_{1k}=\chi^{(+)}(q_k),\quad A_{2k}=\chi^{(-)}(q_k),$$

$$A_{3k}=\gamma_k\chi^{(+)}(q_k),\quad A_{4k}=\gamma_k\chi^{(-)}(q_k). \tag{27}$$

The four Eqs. (26) determine the unknowns $E_x^{(2)}/E_x^{(1)}$, $E_x^{(3)}/E_x^{(1)}$, $E_x^{(4)}/E_x^{(1)}$, and $E_x^{(5)}/E_x^{(1)}$. These quantities, once expressed in terms of 4×4 determinants, are substituted in Eq. (19). This completes the calculation of the surface impedance of the semiconductor, including a dead layer, for the generalized Mahan-Hopfield ABC.

Instead of assuming that $P_{x,z}^{(+)}$ and $P_{x,z}^{(-)}$ vanish at $z=0$, one may also work with the ABC's that the *normal derivatives* of these polarizations vanish at $z=0$. Formally this results only in a minor change, namely, Eq. (26) must be replaced by

$$\sum_{k=1}^{5}q_kA_{jk}E_x^{(k)}=0,\quad j=1,2,3,4. \tag{28}$$

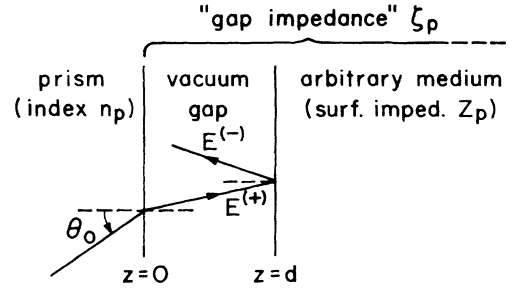

FIG. 2. Schematics of the attenuated total reflection (ATR) geometry employed in Sec. IV. The light is p polarized.

IV. ATTENUATED TOTAL REFLECTIVITY (ATR)

We will now calculate the ATR, in the Otto geometry, of an isotropic, but otherwise arbitrary medium characterized by a surface impedance Z_p. In the following section we will substitute for Z_p the expression given by Eqs. (18), (19), and (26) [or, Eq. (28) replacing Eq. (26)]. Now, however, the explicit form of Z_p is immaterial. The prism-gap-medium configuration is shown in Fig. 2. The width of the gap is d.

The surface impedance of the medium is independent of the choice of the origin; here it is convenient to shift the crystalline surface to $z=d$ and replace Eq. (16) by

$$Z_p = E_x(d^+)/B_y(d^+) . \tag{29}$$

We also define a "gap impedance," given by

$$\zeta_p = E_x(0^+)/B_y(0^+) . \tag{30}$$

The p-polarized reflectivity (that is, in our case, the ATR) may be expressed in terms of ζ_p by means of the well-known formula

$$R_p = \left| \frac{\zeta_p - \cos\theta_0/n_p}{\zeta_p + \cos\theta_0/n_p} \right|^2 . \tag{31}$$

Our remaining task is to express ζ_p as a function of the known Z_p.

The fields inside the gap have the same form as Eqs. (12) and (13). However, ϵ_0 must be replaced by unity, and q_l by q_g, defined as

$$q_g = (q_0^2 - q_x^2)^{1/2} = q_0(1 - n_p^2 \sin^2\theta_0)^{1/2} . \tag{32}$$

Then, omitting the factors $\exp[i(q_x x - \omega t)]$, we have

$$E_x^{(g)}(z) = E^{(+)} e^{iq_g z} + E^{(-)} e^{-iq_g z} , \tag{33}$$

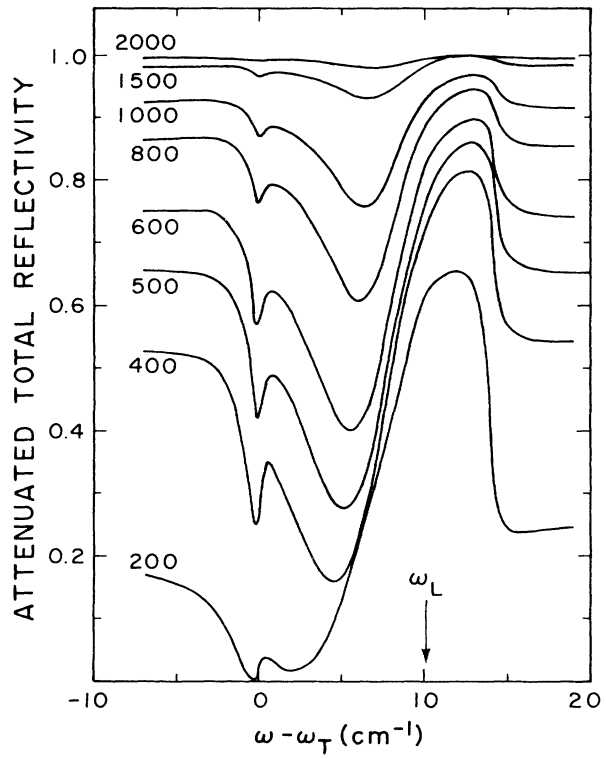

FIG. 3. Attenuated total reflectivity as a function of relative frequency in the vicinity of the B exciton of CdS. The parameters (Ref. 6) are listed in Sec. II (except for the dead-layer thickness $l=70$ Å). The numbers next to each curve are different widths d (in Å) of the gap between the prism and the crystal surface. The broad minima between ω_T and ω_L correspond to the ordinary, "local" surface-exciton polariton. The narrow minima, approximately at ω_T, possibly correspond to a new, "nonlocal" surface-exciton polariton. Notice that, for $d \geq 400$ Å, the positions of the latter minima remain practically unchanged.

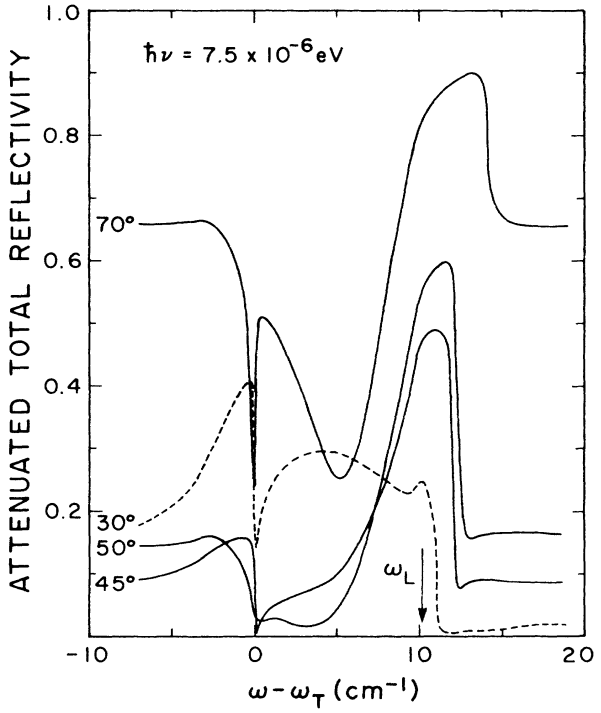

FIG. 4. As in Fig. 3, however with a reduced damping frequency, $\hbar\nu = 7.5\times10^{-6}$ eV, and $d=500$ Å. The numbers next to each curve are angles of incidence θ_0 at the interface between the prism and the gap. The dashed curve, for an angle of incidence that is smaller than the critical angle θ_c ($\simeq 42°$) cannot correspond to the excitation of surface polaritons.

$$B_y^{(g)}(z)=\frac{q_0}{q_g}(E^{(+)}e^{iq_g z}-E^{(-)}e^{-iq_g z}) . \tag{34}$$

Substituting these expressions in Eq. (30) we find that

$$\zeta_p=\frac{q_g}{q_0}\frac{1+r}{1-r},\quad r=\frac{E^{(-)}}{E^{(+)}} . \tag{35}$$

Because of the continuity of E_x and B_y at the interface $z=d$ the right-hand side of Eq. (29) may be also expressed in terms of Eqs. (33) and (34), as follows

$$Z_p=E_x^{(g)}(d)/B_y^{(g)}(d)$$
$$=\frac{q_g}{q_0}\frac{1+r\exp(-2iq_g d)}{1-r\exp(-2iq_g d)} . \tag{36}$$

By eliminating r from Eqs. (35) and (36) we find the desired relation,

$$\zeta_p=\frac{Z_p-i(q_g/q_0)\tan(q_g d)}{1-i(q_0/q_g)Z_p\tan(q_g d)} . \tag{37}$$

This substituted in Eq. (31) gives the ATR in terms of Z_p, n_p, d, and θ_0.

V. RESULTS AND DISCUSSION

We have calculated the ATR for the B exciton of CdS using the material parameters listed in Sec. II and a thickness $l=70$ Å for the dead layer. As a check on our calculations the prism has been "removed" by taking $n_p=1$; then for $\theta=1°$ we reproduce the Mahan-Hopfield results for normal-incidence reflectivity. In all the other calculations the prism index is $n_p=1.5$. In Fig. 3 we show the ATR spectra for an angle of incidence $\theta_0=70°$ and a

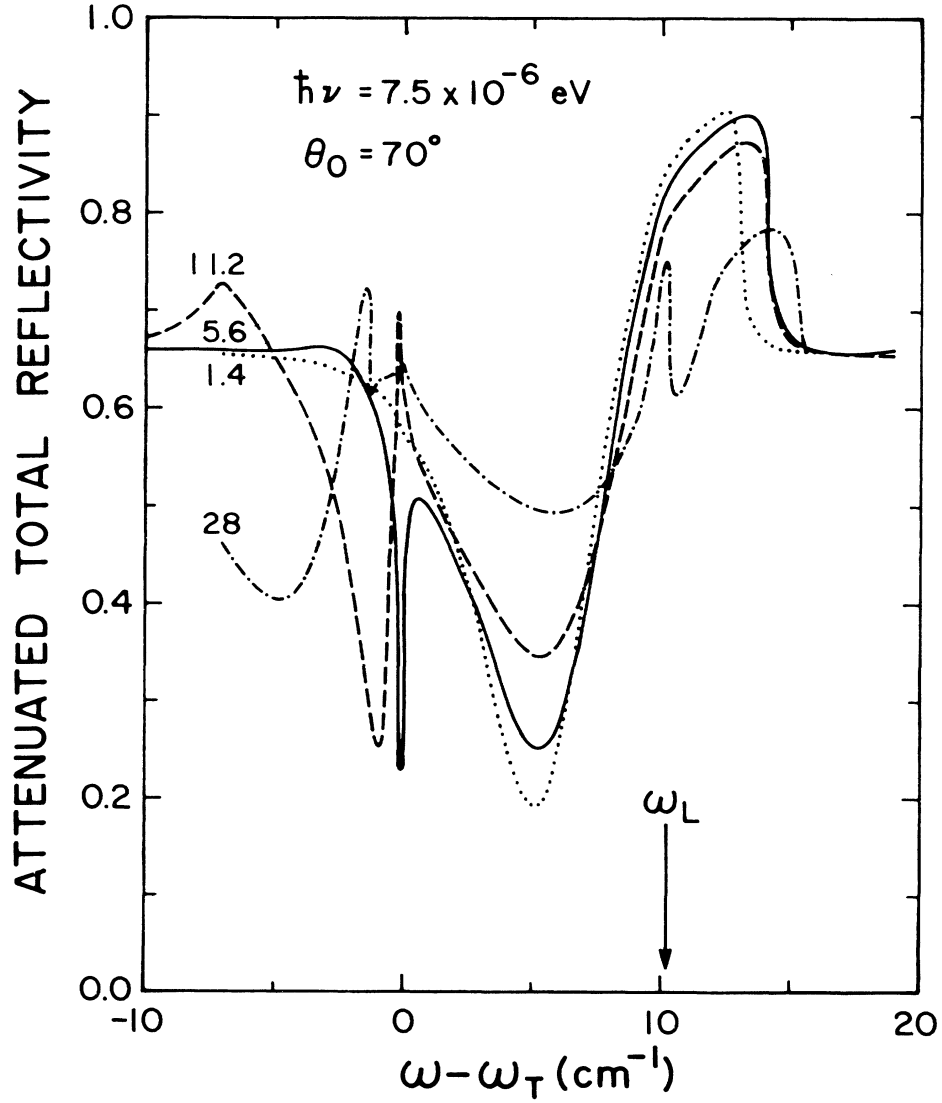

FIG. 5. As in Fig. 3, however with a reduced damping frequency, $\hbar\nu=7.5\times10^{-6}$ eV, and $d=500$ Å. The numbers next to each curve are different values of the splitting parameter ϕ in (10^{-12} eV m). Note that, for $\phi=1.4\times10^{-12}$ eV m only the minimum corresponding to the ordinary surface polariton appears.

series of separations d between the prism and the surface of the medium. All the curves exhibit one broad minimum between ω_T and ω_L and a narrow minimum approximately at ω_T. The former minima gradually shift to higher frequencies as the gap d is increased. These minima persist even for $\phi \to 0$ and $m \to \infty$, and we interpret them as corresponding to the ordinary ("local") surface-exciton polariton, however modified by the nonlocal effects.[3,23] On the other hand, the narrow minima vanish in the limit $\phi \to 0$ and in Ref. 22 we have proposed that they correspond to a new surface polariton—a direct consequence of the wave-vector-linear splitting. Note that, for $d \geq 500$ Å, the low-frequency minima are located almost exactly at $\omega = \omega_T$. Because the depths of the minima decrease with increasing d, in all the subsequent graphs we have chosen $d = 500$ Å. Also, in order to facilitate the interpretation of the effects of spatial dispersion, in Figs. 4–7 we have reduced the damping frequency to an unrealistically small value, $\hbar\nu = 7.5 \times 10^{-6}$ eV.

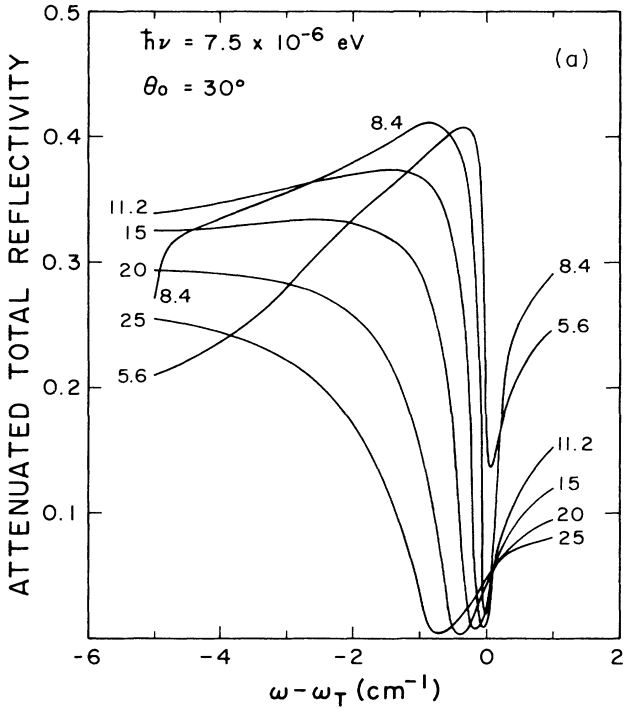

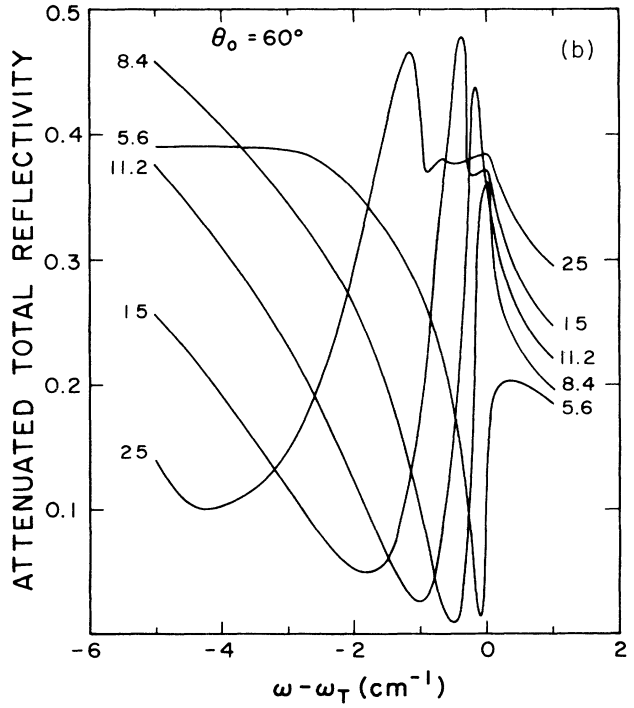

FIG. 6. As in Fig. 5, (a) $\theta_0 = 30°$, (b) $\theta_0 = 60°$.

The spectra shown in Fig. 4 for several angles of incidence are quite similar to those in Fig. 1 of Ref. 22. For $\theta_0 = 50°$ we may still discern two minima; however, for $\theta_0 = 45°$ the broad minimum disappeared, while the narrow minimum changed into a shape that is rather uncharacteristic of ATR minima. The critical angle for the prism air interface is $\theta_c \simeq 42°$. A minimum at $\omega \simeq \omega_T$ still exists even for $\theta_0 = 30°$, well below θ_c; however, this minimum certainly does not describe a surface polariton. (See also Fig. 2 of Ref. 22.)

In order to investigate further the nature of the lower-frequency ATR minimum, in Fig. 5 we vary the value of the q-linear parameter ϕ from 1.4×10^{-12} eV m to 28×10^{-12} eV m. For $\phi = 1.4 \times 10^{-12}$ eV m the narrow, lower-frequency dip is absent and only the broad minimum between ω_T and ω_L appears. This confirms our statement that the narrow line is caused by the q-linear splitting whereas the broad minimum corresponds to the ordinary surface-exciton polariton. For $\phi = 2.8 \times 10^{-12}$ eV m (not shown in Fig. 5) the lower-frequency dip is al-

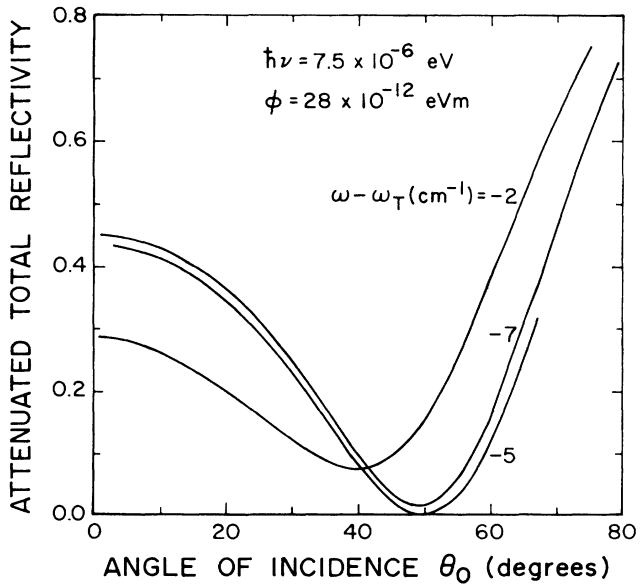

FIG. 7. Angular scan: attenuated total reflectivity as a function of the angle of incidence θ_0 at the interface between the prism and the gap. The numbers next to the curves indicate the difference $\omega - \omega_T$ in cm^{-1}. The parameters are as in Fig. 3, however $\hbar\nu = 7.5 \times 10^{-6}$ eV and $\phi = 28 \times 10^{-12}$ eV m.

ready present, and the spectrum is quite similar to the one for $\phi = 5.6 \times 10^{-12}$ eV m (the same as in Fig. 4 for $\theta_0 = 70°$); the dip is just a little above ω_T. If we increase ϕ further, to 11.2×10^{-12} eV m, the position of the ordinary surface-exciton polariton resonance is almost unaffected; however, the width of the minimum increases considerably. At the same time the new resonance line moves 1 cm^{-1} to lower frequencies and also becomes much wider. For $\phi = 28 \times 10^{-12}$ eV m the lower-frequency minimum has shifted ~ 5 cm^{-1} to the left of ω_T and its width has become comparable to that of the higher-frequency minimum. There is also some additional structure, to which we do not attach major importance on account of the unrealistically high value of ϕ for this curve.

We should comment that minima in the ATR spectrum below ω_T are obtained even for the angles well below the critical angle $\theta_c = 42°$, and even for normal incidence. These minima certainly do not correspond to surface polaritons because, for $\theta < \theta_c$, the normal component of the vacuum wave vector is real. In Figs. 6(a) and 6(b) we compare spectra for $\theta_0 = 30°$ and $\theta_0 = 60°$ in the region $\omega \lesssim \omega_T$. The variation of ϕ has a much stronger effect in Fig. 6(b). Similar graphs have been also obtained in Ref. 22 (Fig. 3) for $\hbar v = 7.5 \times 10^{-5}$ eV.

We have also done ATR calculations with an angular scan, selecting a high value of the splitting constant, $\phi = 28 \times 10^{-12}$ eV m. In Fig. 7 we observe deep and broad minima for three values of ω, all considerably lower than ω_T. For $\omega = \omega_T - 5$ cm^{-1} the minimum is positioned at $\theta_m = 50°$. This roughly corresponds to the minima resulting from a frequency scan, Fig. 2 of Ref. 22. There, for the same value of ϕ and three values of θ_0 (45°, 70°, and 85°), the lower-frequency minimum was obtained, approximately, at $\omega_T - 5$ cm^{-1}. Thus the positions of the minima in the frequency-scan spectra are very insensitive to θ_0. Then we would expect that a small change in ω would produce a large change in the position of the angular-scan minimum. However, curiously, practically the same θ_m is obtained for $\omega - \omega_T = -5$ and -7 cm^{-1}. For a higher frequency $\omega - \omega_T = -2$ cm^{-1}, we find that $\theta_m = 40° < \theta_c$. With realistic values of θ and ν (as in Fig. 3 and Fig. 1 of Ref. 22) and $\omega - \omega_T = +5$ cm^{-1} we find a broad minimum centered at $\theta_m = 54°$ that obviously corresponds to the "local surface-exciton polariton." With the same parameters and $\omega - \omega_T = -0.5$ or 0 cm^{-1} the corresponding minima are both centered at $\theta_m = 51°$. These minima seem to describe the "nonlocal surface-exciton polariton".

Figures 3–7 are all based on the ABC's that $P^{\pm}_{x,z}(z)$ vanish at the interface between the nonlocal bulk and dead layer. These four conditions are given by Eqs. (20) and (21) or, more compactly, by Eq. (26). It is interesting to repeat the calculation with another set of ABC's, namely the vanishing of $\partial P^{\pm}_{x,z}/\partial z$ at the above-mentioned interface, given by Eq. (28). The results are shown in Fig. 8, for the same set of parameters as in Fig. 3 and $d = 500$ Å. The dashed curve is the same as the one labeled $d = 500$ Å in Fig. 3 and is given for comparison. We see that the positions of both minima are almost the same for the two sets of ABC's. However the minimum between ω_T and ω_L is considerably narrower, and the minimum at ω_T is much less deep for the ABC's Eq. (28). This indicates

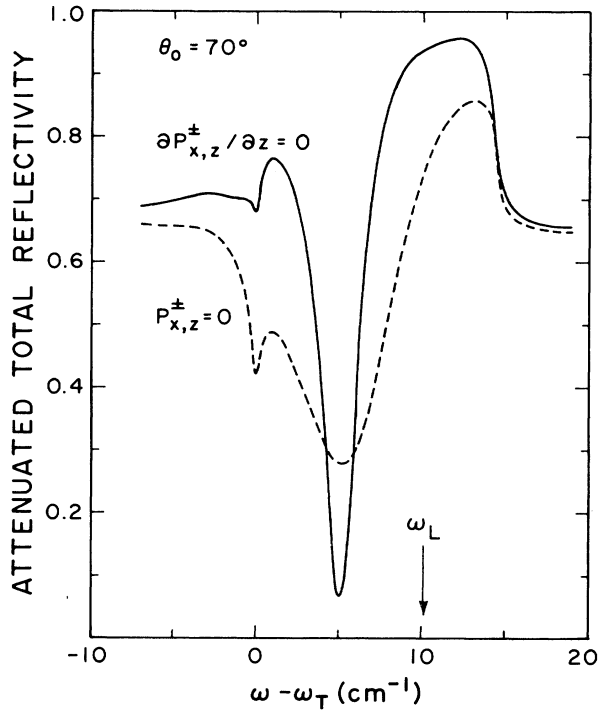

FIG. 8. Comparison of two sets of additional boundary conditions (ABC's). The solid line is based on the ABC that the normal derivatives of the four polarization components $P^{\pm}_{x,z}(z)$ vanish at the interface between the nonlocal bulk and the exciton-free surface layer. The dashed curve has been calculated with the ABC that the polarization components $P^{\pm}_{x,z}(z)$ themselves vanish at this interface. The parameters are the same as in Fig. 3 and $d = 500$ Å.

that spatial dispersion plays a much more important role in the case of the generalized Mahan-Hopfield ABC, Eq. (26).

VI. CONCLUSION

Do the additional ATR minima, obtained for $\theta_0 > \theta_c$, describe surface polaritons? For $\theta_0 > \theta_c$ the wave fields in the gap between the prism and the surface decrease (roughly exponentially) away from the surface. The imposition of the conditions $\mathrm{Im} q_k \geq 0$ ensures that the total wave fields (composed of the five partial modes) decay in amplitude away from the interface between the bulk medium and the surface layer (except in the case, unlikely for $\nu \neq 0$, that $\mathrm{Im} q_k$ vanishes for some k and ω). Thus it seems—almost by definition—that for $\theta_0 > \theta_c$ *any* ATR *minimum* corresponds to some surface polariton mode. This is true in simple cases. However, here we are dealing with a rather complex model. If the decay of the *total* wave fields is very slow (on the scale of the vacuum wavelength, say) then an ATR minimum can hardly represent *bona fide* surface modes.

A glance at Fig. 1 reveals that $\mathrm{Im} q_1$ is smaller than ω_T/c over the complete range of interest. So, the partial bulk mode $k = 1$ is certainly removing energy from the

surface. However, our numerical calculations show that the amplitude of the mode $k=1$ is quite small compared to the amplitudes of the other four modes. Therefore the partial mode $k=1$ is not expected to make an important contribution. For this reason we believe that the additional ATR minima in Figs. 3—8 (for $\theta_0 > \theta_c$ and $\omega \lesssim \omega_T$) corresond to *leaky* surface-exciton-polaritons, and they are certainly a direct consequence of the wave-vector-linear energy bands. We note that, even for $\phi=0$, as a result of a finite exciton mass, surface-exciton-polaritons *are* leaky waves.[3,23]

There should be no difficulty in observing experimentally the ATR spectra calculated in this work. As for the identification of the additional ATR minima with a "nonlocal surface polariton," further theoretical work is needed. Currently the dispersion relation for the semiconductor vacuum interface is being studied.

ACKNOWLEDGMENTS

This work was supported in part by the cooperative research program of the United States and Mexico (Consejo Nacional de Ciéncia y Tecnológia) through National Science Foundation Grant No. INT83-12955.

[1]G. D. Mahan and J. J. Hopfield, Phys. Rev. **135**, A428 (1964).

[2]T. M. Mashlyatina, D. S. Nedzvetskii, and A. V. Sel'kin, Pis'ma Zh. Eksp. Teor. Fiz. **27**, 573 (1978) [JETP Lett. **27**, 539 (1978)].

[3]See, for example, S. I. Pekar, Zh. Eksp. Teor. Fiz. **33**, 1022 (1958); **34**, 1176 (1958) [Sov. Phys.—JETP **6**, 785 (1958); **7**, 813 (1958)]; J. J. Hopfield and D. G. Thomas, Phys. Rev. **132**, 563 (1963); A. A. Maradudin and D. L. Mills, Phys. Rev. B **7**, 2787 (1973); P. Halevi and G. Hernandez-Cocoletzi, Phys. Rev. Lett. **48**, 1500 (1982); P. Halevi and R. Fuchs, J. Phys. C **17**, 3869 (1984).

[4]R. G. Ulbrich and C. Weisbuch, Phys. Rev. Lett. **38**, 865 (1977); G. Winterling and E. S. Koteless, Solid State Commun. **23**, 95 (1977); G. Winterling, E. S. Koteless, and M. Cardona, Phys. Rev. Lett. **39**, 1286 (1977).

[5]N. Allen and E. O. Kane, Solid State Commun. **28**, 965 (1978).

[6]E. S. Koteles and G. Winterling, J. Lumin. **18/19**, 267 (1979); Phys. Rev. Lett. **44**, 948 (1980).

[7]E. S. Koteles, in *Excitons*, edited by E. I. Rashba and M. D. Sturge (North-Holland, Amsterdam, 1982), p. 83.

[8]X. Z. Lu, M. Dutta, and H. Z. Cummins, Phys. Rev. B **33**, 2945 (1986).

[9]T. Shinegari, X. Z. Lu, and H. Z. Cummins, Phys. Rev. B **30**, 1962 (1984); X. Z. Lu, M. Dutta, T. Shinegari, and H. Z. Cummins, *ibid.* **32**, 1037 (1985).

[10]N. T. Thang and G. Fishman, Phys. Rev. B **31**, 2404 (1985).

[11]G. Blattner, G. Kurtze, G. Schmieder, and G. Klingshirn, Phys. Rev. B **25**, 7413 (1982).

[12]M. Rosenzweig, Phys. Status Solid B **129**, 187 (1985).

[13]V. M. Agranovich and V. L. Ginzburg, *Spatial Dispersion in Crystal Optics and the Theory of Excitons* (Wiley, New York, 1966).

[14]E. L. Ivchenko, S. A. Permogorov, and A. V. Sel'kin, Pis'ma Zh. Eksp. Teor. Fiz. **27**, (1978) [JETP Lett. **27**, 24 (1978)].

[15]E. L. Ivchenko and A. V. Sel'kin, Zh. Eksp. Teor. Fiz. **76**, 1836 (1979) [Sov. Phys.—JETP **49**, 933 (1979)].

[16]G. E. Pikus and G. L. Bir, Fiz. Tekh. Poluprovodn. **7**, 119 (1973) [Sov. Phys.—Semicond. **7**, 81 (1973)].

[17]A. B. Pevtsov and A. V. Sel'kin, Fiz. Tverd. Tela **25**, 157 (1983) [Sov. Phys.—Solid State **25**, 85 (1983)].

[18]E. L. Ivchenko, A. B. Pevtsov, and A. V. Sel'kin, Solid State Commun. **39**, 453 (1981).

[19]E. L. Ivchenko, in *Excitons*, Ref. 7, p. 141.

[20]M. F. Bishop and A. A. Maradudin, Solid State Commun. **23**, 507 (1977).

[21]W. Dreybrodt, K. Cho, S. Suga, F. Willman, and Y. Niji, Phys. Rev. B **21**, 4692 (1980); Y. Nozue, M. Itoh, and K. Cho, J. Phys. Soc. Jpn. **50**, 889 (1981); M. S. Brodin, V. M. Bandura, and M. G. Matsko, Phys. Status Solidi B **125**, 613 (1984).

[22]P. Halevi, O. B. M. Hardouin Duparc, A. A. Maradudin, and R. F. Wallis, Phys. Rev. B **32**, 6986 (1985).

[23]See, for example, M. Bishop, A. A. Maradudin, and D. L. Mills, Phys. Rev. B **14**, 4744 (1976); J. Lagois and B. Fischer, Adv. Solid State Phys. **18**, 197 (1978); P. Halevi and R. Fuchs, J. Phys. C **17**, 3889 (1984).